

Supplementary Materials for

Sculpting stable structures in pure liquids

Tadej Emeršič, Rui Zhang, Žiga Kos, Simon Čopar, Natan Osterman, Juan J. de Pablo*, Uroš Tkalec*

*Corresponding author. Email: depablo@uchicago.edu (J.J.d.P.); uros.tkalec@mf.uni-lj.si (U.T.)

Published 15 February 2019, *Sci. Adv.* **5**, eaav4283 (2019)

DOI: 10.1126/sciadv.aav4283

The PDF file includes:

Fig. S1. Universality of the dowser domain annihilation dynamics at small radii.

Fig. S2. Velocity dependence of parameter a from Eq. 3 for the dowser domain size, as extracted from Fig. 2F.

Fig. S3. An independent study, performed in 400- μm -wide and 15- μm -deep channels, shows equivalent behavior of dowser domain dynamics as is discussed in the main text.

Fig. S4. Dowser field relaxation dynamics.

Legends for Movies S1 to S7

Other Supplementary Material for this manuscript includes the following:

(available at advances.sciencemag.org/cgi/content/full/5/2/eaav4283/DC1)

Movie S1 (.mp4 format). Laser tweezers-induced nucleation of the dowser domains in a pressure-driven nematic microflow.

Movie S2 (.mp4 format). Expansion and contraction of laser-nucleated dowser domains in a moderate nematic microflow.

Movie S3 (.mp4 format). Growing and shrinking dowser domains in numerically simulated nematic microflows.

Movie S4 (.mp4 format). A steady stream of dowser domains is produced by chopping the bulk dowser state with a moving laser spot.

Movie S5 (.mp4 format). A growing dowser domain is longitudinally split into two by a static laser spot.

Movie S6 (.mp4 format). Dowser domain reconfiguration under an oscillatory flow.

Movie S7 (.mp4 format). Relaxation dynamics of dowser domains after shutting off the flow.

Supplementary Figures

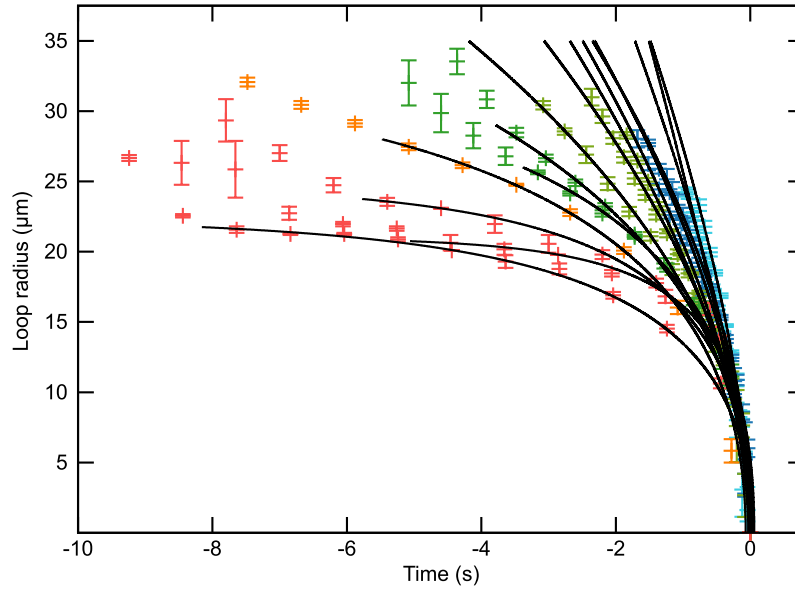


Fig. S1. Universality of the dowser domain annihilation dynamics at small radii. Experimental data points and the corresponding theoretical curves for the shrinking defect loop dynamics in Fig. 2F can be time-shifted to align the annihilation times, showing universal behaviour at small radii, when loop dynamics is governed primarily by the elasticity effects.

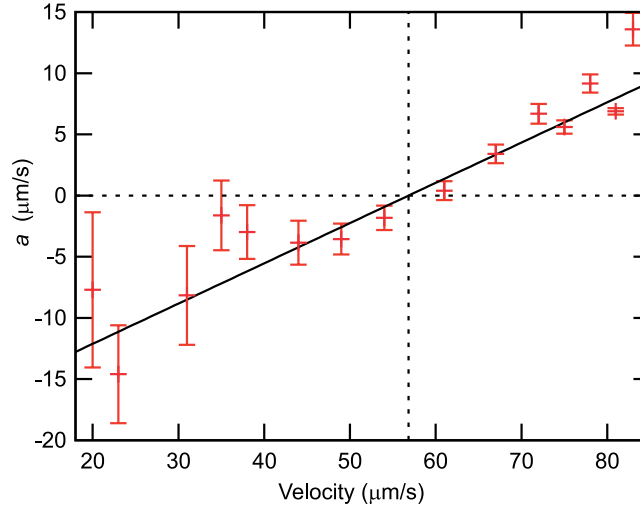


Fig. S2. Velocity dependence of parameter a from Eq. 3 for the dowser domain size, as extracted from Fig. 2F. A critical velocity of $v_c = (56.8 \pm 1.2) \mu\text{m/s}$ is extracted from the linear fit, which corresponds well to the value of v_c obtained in Fig. 2G.

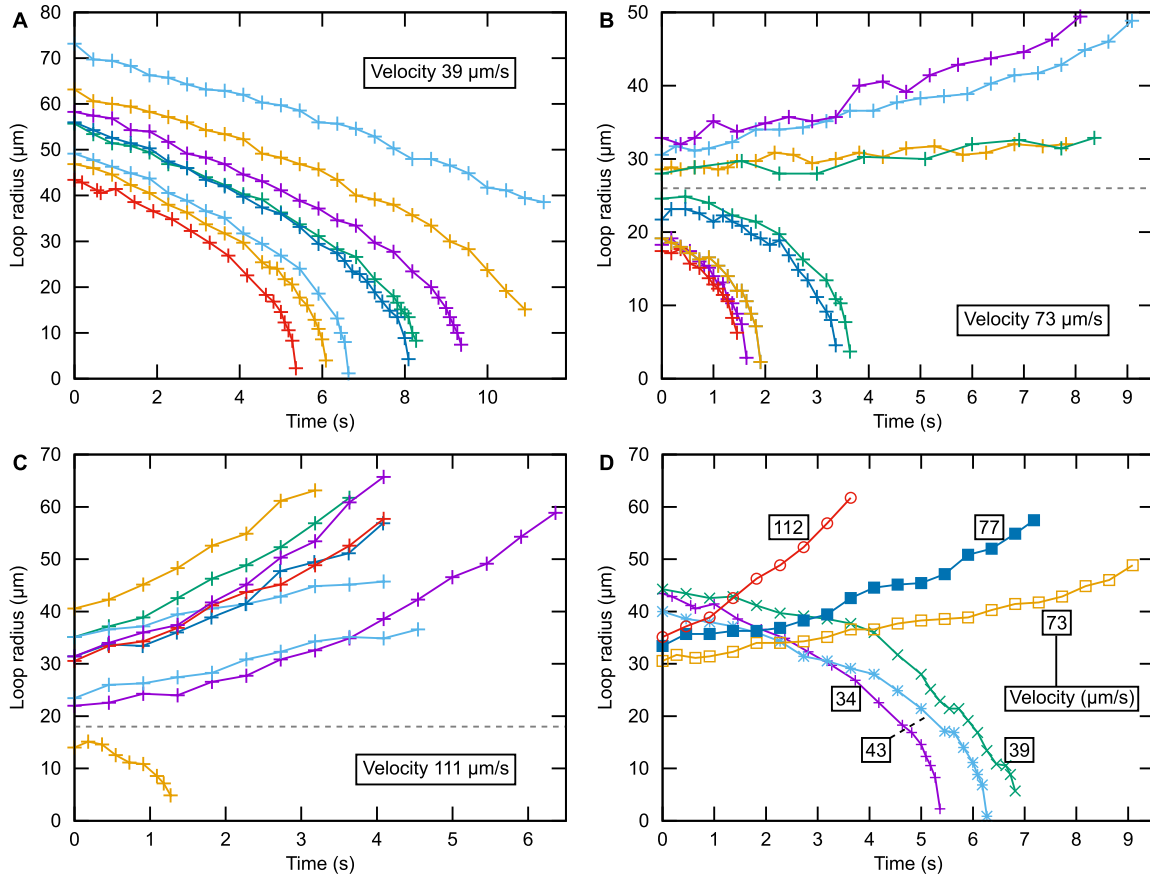


Fig. S3. An independent study, performed in $400\text{-}\mu\text{m}$ -wide and $15\text{-}\mu\text{m}$ -deep channels, shows equivalent behavior of dowser domain dynamics as is discussed in the main text. (A-C) Time dependence of the domain radius for three different flow velocities. Dowser domains with the initial radius above the critical size (approximate value is shown by the dashed line) grow, whereas domains below the critical size shrink. (D) At similar initial sizes, domains in flows with low velocity shrink, while domains at large flow velocity grow in time. Solid lines are added to guide the eye.

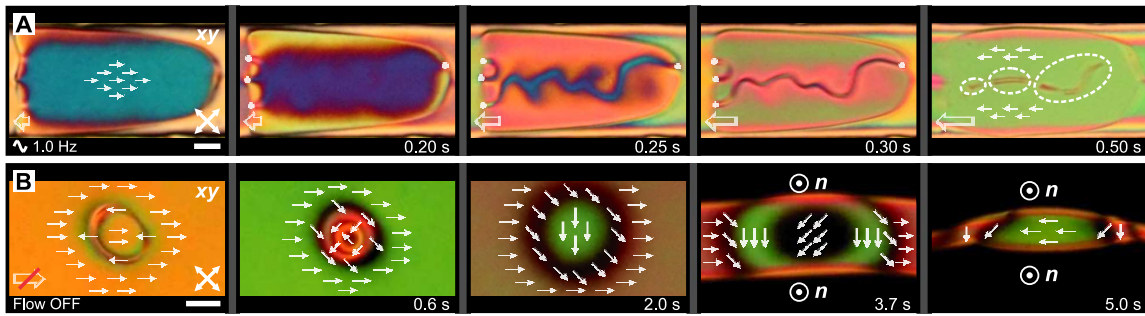


Fig. S4. Dowser field relaxation dynamics. (A) For sufficiently rapid flow rate changes, the director reversal behaves as a quench. It is instantaneous across the entire domain and leads to a nucleation of irregularly shaped solitons, which coarsen over time. While the solitons are topologically protected, they disappear when the characteristic length is so small that a discontinuous director rearrangement becomes possible (dashed ellipses). This scenario effectively represents a local breakdown or “melting” of the dowser alignment, which happens in a fraction of a second. **(B)** A closed circular soliton unwinds and enlarges in a process akin to diffusion of orientational order after shutting off the flow, as Eq. (1) reduces to a diffusion equation in the absence of flow. A slight transient increase of the winding angle is observed in the fourth panel, due to a rebound of the liquid flow, which makes the leftward orientation preferable, as also suggested by the bulbous shape in the final panel. Scale bars, $20 \mu\text{m}$.

Supplementary Movie Captions

Movie S1. Laser tweezers-induced nucleation of the dowser domains in a pressure-driven nematic microflow. Recorded under crossed polarizers at 30 fps. The laser lighting repetition rate was 1.5 s at 150 mW of power and the flow velocity was close to $90 \mu\text{m/s}$. The channel width is $100 \mu\text{m}$ and the channel depth is $12 \mu\text{m}$.

Movie S2. Expansion and contraction of laser-nucleated dowser domains in a moderate nematic microflow. The lifetime of the domain is proportional to the critical velocity and the initial size. Recorded under crossed polarizers at 30 fps. The view field size is $480 \mu\text{m} \times 120 \mu\text{m}$.

Movie S3. Growing and shrinking dowser domains in numerically simulated nematic microflows. Simulation of a laser-induced defect loop in a channel undergoing either expansion or shrinkage, subject to a strong and a weak pressure-driven flow, respectively. Top: top view of the channel showing defect loop. Bottom: side view showing the evolution of dowser structure. Elastic constants of 5CB are adopted in the calculation.

Movie S4. A Steady stream of dowser domains is produced by chopping the bulk dowser state with a moving laser spot. By moving an isotropic island of laser-heated nematic phase transversely across the phase boundary between the dowser and the bowser state one can produce a uniform train of the dowser domains. Recorded under crossed polarizers at 30 fps. The view field size is $480 \mu\text{m} \times 120 \mu\text{m}$.

Movie S5. A growing dowser domain is longitudinally split in two by a static laser spot. The flowing dowser domain is slowed down and halved while traversing a laser beam-generated obstacle. The flow velocity is very close to transition from the bowser to the dowser bulk regime. Recorded under crossed polarizers at 30 fps. The view field size is $480 \mu\text{m} \times 120 \mu\text{m}$.

Movie S6. Dowser domain reconfiguration under an oscillatory flow. A single dowser domain is nucleated by the laser-tweezers-induced isotropic-to-the-nematic phase transition and driven under oscillatory nematic flow. The domain reverses orientation every 3 s as the flow smoothly reverses its direction. One can observe rapid color changes under crossed polarizers when the energetically unfavourable orientation shrinks into a narrow 2π soliton that pinches the domain boundary. The view field size is $480 \mu\text{m} \times 120 \mu\text{m}$.

Movie S7. Relaxation dynamics of dowser domains after shutting off the flow. Turning off the flow leads to a nucleation of solitons which coarsen over time. One can observe the dynamics of point defects, connected by a linear soliton, and their signature profile. In addition, closed circular solitons can appear at abrupt stopping of the flow. These solitons gradually unwind and enlarge in a process akin to diffusion of the orientational order. Recorded under crossed polarizers at 30 fps. The view field size is $360 \mu\text{m} \times 120 \mu\text{m}$.